Annals of the Academy of Romanian Scientists
Series on Engineering Sciences
ISSN online 2066 – 8570 Volume **8**, Number **2**/**2016**

ENERGY MANAGEMENT OF PHOTOVOLTAIC SYSTEMS USING FUEL CELLS

Cristian MIRON[1], Severus Constantin OLTEANU[2],
Catalin PETRESCU[3], Abdel AITOUCHE[4]

Rezumat. *Sistemele energetice regenerabile beneficiază de o creştere accelerată atât în domeniul producţiei comerciale cât şi în domeniul cercetării. Sursele de energie fotovoltaice cât şi eoliene prezintă inconvenientul unui flux energetic întrerupt în funcţie de condiţiile de mediu. Soluţia clasică este de a se crea o reţea între câmpurile de panouri solare pe distanţe mari, care să împartă energia totală generată înainte de a o furniza către utilizatori. O soluţie recent pusă sub analiză este stocarea surplusului energetic pe bază de hidrogen. Pilele de combustie (PdC) sunt generatoare de energie al căror vector energetic uzual este hidrogenul. Acestea au început deja tranziţia de la mediul de laborator la comercializare. Datorită densităţii energetice mari cât şi a capacităţii de stocare teoretic infinită prin hidrogen, acestea se prezintă ca un sistem de stocaj cu înalt potenţial, atât în aplicaţii mobile cât şi în aplicaţii staţionare. Astfel studiul asupra acestor tipuri de sisteme de control distribuit prezintă o importanţă ridicată. Această lucrare analizează soluţiile existente, punând accentul pe un caz particular.*

Abstract. *Renewable energy generators show an accelerated growth both in terms of production wise, as well as in research fields. Focusing only on photovoltaic panels, the generated energy has the disadvantage of being strongly oscillatory in evolution. The classical solution is to create a network between photovoltaic farms spanning on large distances, in order to share the total energy before sending it to the clients. A solution that was recently proposed is going to use hydrogen in order to store the energy surplus. Fuel Cells (FCs) represent energy generators whose energy vector is usually hydrogen. These have already started the transition from the laboratory context towards commercialization. Due to their high energy density, as well as their theoretical infinite storage capacity through hydrogen, configurations based on electrolyzers and FCs are seen as high potential storage systems, both for vehicle and for stationary applications. Therefore, a study on such distributed control systems is of high importance. This paper analyses the existing solutions, with emphasis on a particular case where a supervisory system is developed and tested in a specialised simulation software.*

Keywords: control systems, renewable energy, energy management, fuel cells, photovoltaic energy

[1]Eng., University of Lille 1, Villeneuve D'Ascq, France (arh_cristi@yahoo.com).
[2]Junior Researcher, Faculty of Automatic Control and Computer Science, University *Politehnica* of Bucharest, Romania (severus.olteanu@gmail.com).
[3]Prof., Faculty of Automatic Control and Computer Science, University *Politehnica* of Bucharest, Romania.
[4]Prof., Cristal research Laboratory, Hautes Etudes d'Ingenieur School of Engineering, Lille, France.

1. Introduction

As the conventional energy sources started depleting, the popularity of renewable sources increased significantly during the last decades. The policy of the European Union regarding the production of energy encouraged this alternative.

Since the energy provided by the sun should be sufficient to cover the entire world's energy consumption, if captured and stored at reasonable costs, the use of photovoltaic panels will have an increased popularity in time. The "green energy" sector comes with new challenges such as low conversion rates, additional energy storage systems and transfer inefficiency between the PV array and its connected load.

Photovoltaic power stations up to 500 kW both in isolated areas and in urban zones will have an exponential development, as many countries reorient their policies regarding the production of energy embracing the use of "green energy".

As such, the global tendency is to promote the concepts of energy optimization and energy independence through renewable sources, and among these, the photovoltaic panels are the most favourable. In this sense, the European Union has set the directive 2010/31/UE, in which, by 2021, all new building should be "nearly zero-energy buildings", suggesting that a significant amount of energy should be covered by renewable sources, local or nearby.

Because PV panels still have a reduced conversion rate, a strong and fast power variation and a wide geographical distribution of PV generators, it is implicitly obvious that an optimal energy management is essential.

There are two important solutions for achieving this: the first one consists in the construction of a large energy grid, spread on geographical regions with variable power generation conditions, whereas the second approach implies the use of Smart Storage solutions [7].

Three main types of storage exist: Mechanical storage, as for example: water pumping systems (ex: storage by water pumping in Ludington: 110 m, 1.87 GW, 15 h, 27 million kWh); battery based solutions with different types of batteries used, each with its own advantages and disadvantages [8], [13]; and, finally, hydrogen based storage, bringing a high energy density, good conversion efficiency and physical robustness [10].

This article focuses on hydrogen storage solutions. Fuel Cells (FC) represent energy generators whose energy vector is hydrogen. They have begun the transition from laboratory research stage towards commercialization, being promoted especially by vehicle production companies, as they come with the advantage of pollution elimination and a fast recharge time compared to batteries. Because of their high energy density, as well as their capability to store high

quantities for indefinite periods, storage systems made of the pair Electrolyser/Fuel Cell Systems (FCS) offer a high potential of being used in stationary applications [9].

The directions and objectives of this article follow the previously discussed problem of photovoltaic energy management by means of storage, where the storage is achieved through Hydrogen based solutions.

The paper also contributes with the demonstration of a simulation in a professional simulator, for a microgrid, that can be potentially adapted to any different type of configuration.

The article presents a description of the components of the hybrid energy system, in Sections II, III, IV and V. This is followed in section VI by a description of the Maximum Power Point Tracking algorithm. Section VII deals with the supervisory management system and the presentation of the simulation platform containing the results thus obtained. The article ends with a set of conclusions.

2. Photovoltaic two diode model

As presented in different paperwork [1]-[5], the behaviour of a photovoltaic (PV) cell can be achieved using various mathematical models. A certain degree of accuracy will be obtained according to the complexity of the PV cell model.

The main differences between these models can be noticed by analysing the non-linear characteristic curves, I-V and P-V.

By connecting a current source (Iph) in parallel to a diode (D_1), the output current (Ipv) of an ideal PV cell can be obtained.

The advantage of this model consists in its simplicity, it requires just three parameters in order to compute the I-V characteristic curve – an open circuit-voltage (Voc), a short-circuit current and diode ideality factor (α).

Nonetheless this model is unsuitable for real world functioning when exposed to environmental variation.

Other models are obtained from the previous one. Adding a series resistance (Rs) generates one of the most frequently used models in the specialized literature. Adding a parallel resistance (Rp) to the latter model we gain even more precision.

However, the previous two models encounter a lack of precision when exposed to temperature variations (the Rs model) and to low voltages (the Rs model), due to the recombination losses that are not taken into consideration.

These inconveniencies are avoided by adding another diode to the structure of the Rp model, obtaining the model of a double diode PV cell as presented in Figure 1.

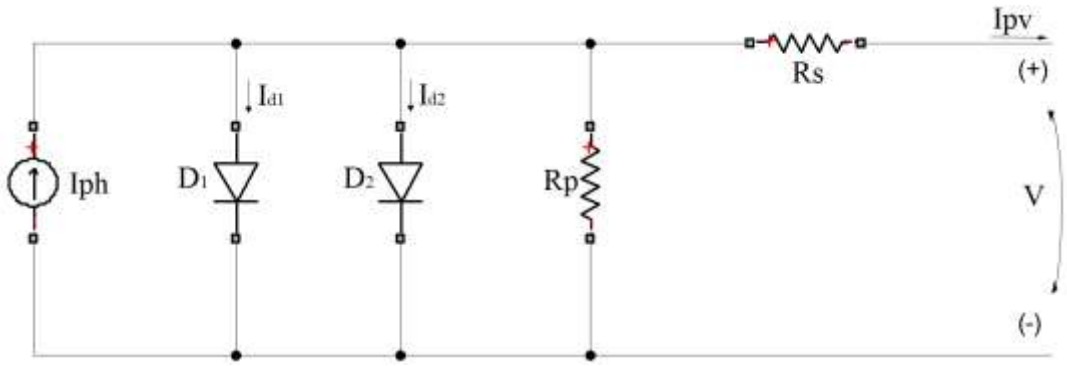

Fig.1. PV cell model.

The output current (I_{pv}) equation of the PV module can be expressed as below:

$$I_{pv} = I_{ph} - I_{d1} - I_{d2} - \left(\frac{V + I_{pv}R_s}{R_p}\right) =$$

$$= I_{ph} - I_{01}\left[e^{\frac{V+I_{pv}R_s}{\alpha_1 V_{T1}}} - 1\right] - I_{02}\left[e^{\frac{V+I_{pv}R_s}{\alpha_2 V_{T2}}} - 1\right] - \left(\frac{V+I_{pv}R_s}{R_p}\right) \quad (1),$$

where:

I_{pv} is the output current of the PV cell; I_{ph} is the photo generated current by the incidence of light; V is the output voltage of the PV cell; I_{d1} is the diffusion diode current (obtained with the Shockley diode equation) ; I_{d2} is the recombination diode current; I_{01} and I_{02} are the reverse saturation currents or leakage currents of the diode D_1,respectively D_2; V_{T1} and V_{T2} are the thermal voltages of the two diodes ,$V_T = \frac{k_b}{q}T$, where k_b is the Boltzmann constant ($1.380650 * 10^{-23} J/K$), q is the electron charge ($1.602176 * 10^{-19} C$) and T is the temperature of the p-n junction (in Kelvin) ;α_1 and α_2 are the ideality factors of the two diodes; R_s is a series resistance; R_p is a shunt resistance.

Furthermore, the expression of the light generated current can be written as:

$$I_{ph} = \left(I_{ph\_STC} + K_i \Delta T\right)\frac{G}{G_{STC}}. \quad (2),$$

where I_{ph_STC} is a light generated current measured in standard test conditions (STC) - $irradiance = 1000\ W/m^2$ and $temperature = 298.15\ K$, K_i $[mA/K]$ is the short circuit current coefficient, $\Delta T = T - T_{STC}$ [K], G is the irradiance, while G_{STC} is the irradiance measured in STC.

The following formula (4) of the reverse saturation current of the diode is preferred to the classical one (3):

$$I_0 = I_{0,STC}\left(\frac{T_{STC}}{T}\right)^3 e^{\left[\frac{qE_g}{\alpha k_b}\left(\frac{1}{T_{STC}}-\frac{1}{T}\right)\right]}, \quad (3)$$

where Eg is the band gap energy of the semiconductor and $I_{0,STC}$ is the reverse saturation current at STC.

$$I_0 = \frac{(I_{sc\_STC}+K_i\Delta T)}{e^{[(V_{oc,STC}+K_v\Delta T)/(\alpha V_T)]}-1} \quad (4),$$

where $K_v[mV/K]$is the open circuit current coefficient and $V_{oc,STC}$ is the open circuit voltage at STC. In order to compute the characteristic curve seven parameters are required: I_{pv}, I_{01}, I_{02}, R_s, R_p, $\alpha_1$and α_2.

If the following simplification is taken into account [8], the reverse saturation current equations for both diodes become:

$$I_{01} = I_{02} = \frac{(I_{sc\_STC}+K_i\Delta T)}{e^{[(V_{oc,STC}+K_v\Delta T)/V_T]}-1} \quad (5)$$

A solar panel such as FVG100P can be used for many low budget applications.

Having a quick look over the data (Table 1.) that is provided by the manufacturer one can observe that the values of resistances R_s and R_p are not available.

FVG100P PV DATASHEET @STC

Cells in series	36
Maximum rated Power – Pm [W]	9.975
Maximum power Voltage – Vm [V]	17.5
Maximum power Current – Im [A]	0.57
Open Circuit Voltage – VOC [V]	21.00
Short Circuit Current – ISC [A]	0.66
VOC Temperature Coefficient [%/°C]	-0.35
ISC Temperature Coefficient [%/°C]	0.05

A solution for this scenarios is obtained by applying the Newton-Rhapson algorithm for finding the values of R_s and R_p described in [1, 2, 8], adapted for the two diode PV cell model. The following graphic user interface (GUI) was developed to facilitate the computation of the two values (Fig. 2.).

After filling in the gaps with the data provided in the datasheet of the PV panel and choosing a suitable value for α_2 (α_1=1, by default) the button that enables the search algorithm can be pressed. The results will be shown along with the I-V and P-V characteristic curves. The simulation is made for a 1500 watts PV array, as in Figure 2, while the characteristic curves can be observed in Figure 3.

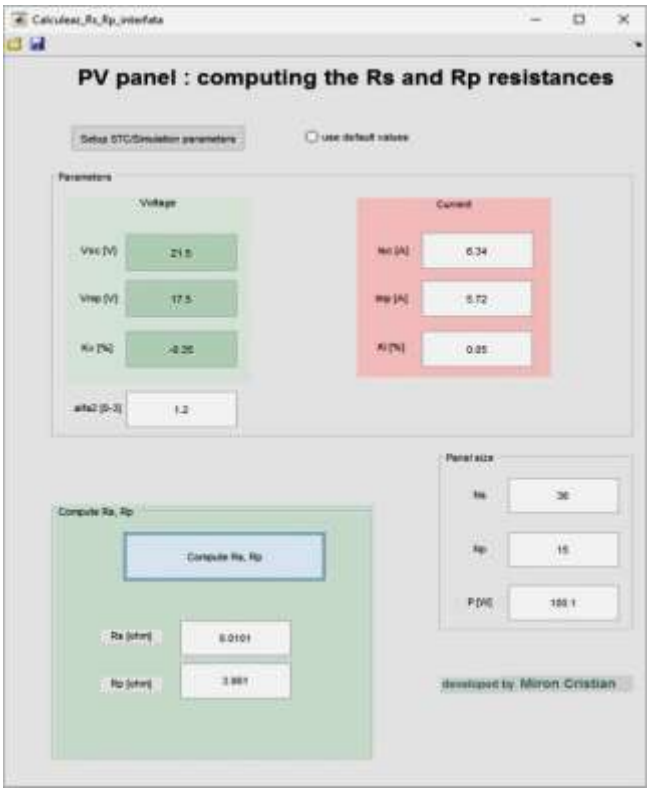

Fig. 2. Graphic User Interface

The computed values are $R_s = 0.0101\Omega$ and $R_p = 3.061\Omega$.

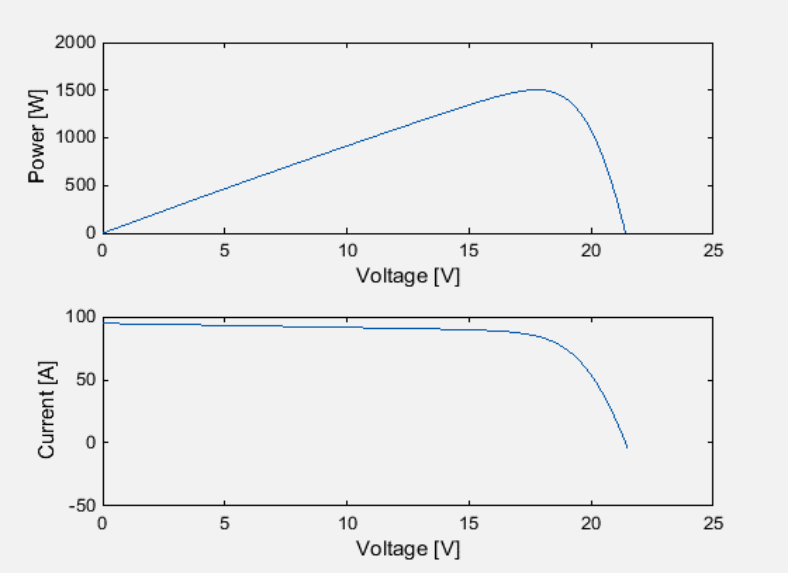

Fig. 3. I-V and P-V characteristic curves.

A PV array can deliver different amounts of energy depending on the meteorological conditions, such as irradiance and temperature, and its load. Therefore, maximum power can be delivered using various maximum power point tracking (MPPT) algorithms. Regardless of the algorithm a certain condition should be fulfilled:

$$\frac{dP}{dV} \cong 0, \tag{6}$$

which can be expressed as:

$$\frac{dP}{dV} = \frac{d(I_{pv}V)}{dV} = I_{pv} + V\frac{dI_{pv}}{dV} = \quad I_{pv} + V\left[-I_{01}N_p\left(\frac{1}{\alpha_1 V_{T1} N_s}\right)e^{\frac{V+IR_s}{\alpha_1 V_{T1}}} - I_{02}N_p\left(\frac{1}{\alpha_1 V_{T1} N_s}\right)e^{\frac{V+IR_s}{\alpha_1 V_{T1}}} - \frac{1}{R_p\left(\frac{N_s}{N_p}\right)}\right] \tag{7}$$

3. DC/DC Buck converter

The following scenario (Fig. 4) is proposed. The PV panel is connected to a load (battery) via a step down converter. The role of the DC-DC buck converter is to increase the efficiency of the PV panel and to deliver the proper voltage to the load.

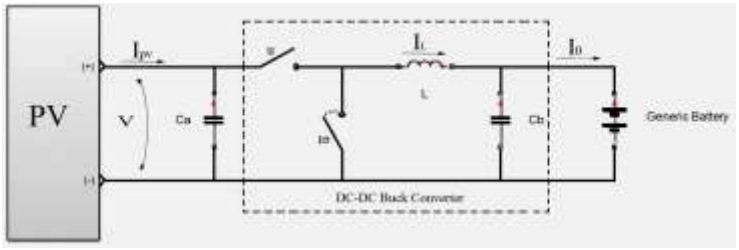

Fig. 4. Step down converter.

The synchronous buck topology is composed of an inductor (L), a capacitor (C_b), and two MOSFET transistors. The control of the converter is achieved using a pulse-width modulation signal (PWM), also called duty ratio u, via the high-side MOSFET, and using the duty ratio $\overline{u}$ via the low-side MOSFET.

Using a second transistor instead of a diode there is a lower resistance from drain to source, increasing thus the efficiency of the topology. The performance of the converter can be measured by analysing if the power is conserved:

$$P_{out\_buck} = P_{in\_buck} + P_{losses} \tag{8}$$

Power dissipation on the inductor or switching losses on the transistors has an impact on the power losses, affecting the amount of produced energy.

4. Electrolyser Unit

In order to obtain the hydrogen by means of electricity, the electrolyser is the most spread solution. There are two main types of electrolysers: PEM electrolysers, that act in a way like a reversed Fuel Cell and alkaline electrolysers, being simpler and a more accessible solution. The energy efficiency of an electrolyser can reach an efficiency of 80% and a 99.5% purity of obtained hydrogen. Here we have considered an alkaline electrolyser: a good reference, on which this article relies, is [11]. The electrolyser is a 1.5 KW model that activates after a certain minimal current is reached. Temperature variation is taken into account, as in (9).

$$U_{elsc,cell} = U_{rev} + \frac{r_{1+}r_2 T}{A} I + k_{elsc} \ln \frac{k_{T1} + \frac{k_{T2}}{T} + \frac{k_{T3}}{T^2}}{A} I + 1) \qquad (9)$$

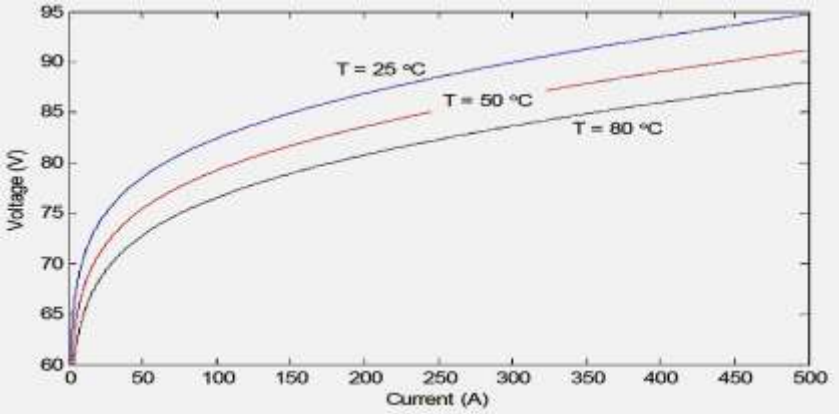

Fig. 5.U-I characteristics of the electrolyser at different temperatures. Graphic User Interface.

The coefficients are computed as follows: r_1 and r_2 are experimentally obtained constants; k_{T1}, k_{T2}, k_{T3} are temperature related constants. U_{rev} is the reversal voltage.

5. Fuel Cell System

FCs are of different types, but two major categories stand out: FCs based on a Proton Exchange Membrane (P.E.M.), and solid oxide FCs. The first class distinguishes itself through low working temperatures (around 100 degrees Celsius), whereas solid oxide may reach 1000 degrees [12]. A PEM FC is chosen in this work.

From a mathematical modelisation point of view, the FC model has two sides: a gaseous part and an electro-chemical part. A detailed modelisation of the gaseous part is done in [14]. This is expressed through the following equations:

$$\frac{dp_{sm}}{dt} = \frac{R_{O_2} \cdot T_{st}}{V_{sm}} \cdot \left(W_{cp} - W_{sm,out}\right)$$
$$\frac{dp_{rm}}{dt} = \frac{R_a \cdot T_{rm}}{V_{rm}} \cdot \left(W_{ca,out} - W_{rm,out}\right)$$
$$\frac{dp_{O_2,ca}}{dt} = \frac{R_{O_2} \cdot T_{st}}{V_{ca}} \cdot \left(W_{O_2,ca,in} - W_{O_2,ca,out} - W_{O_2,reacted}\right) \quad (10)$$
$$\frac{dp_{v,ca}}{dt} = \frac{R_v \cdot T_{st}}{V_{ca}} \cdot \left(-W_{ca,out} + W_{v,ca,gen}\right)$$
$$\frac{dp_{H_2,an}}{dt} = \frac{R_{H_2} \cdot T_{st}}{V_{an}} \cdot \left(W_{H_2,an,in} - W_{H_2,an,out} - W_{H_2,reacted}\right)$$

The electrochemical side, on the other hand is determined by the Nernst equations:

$$V_{dc\_stack} = V_{open} - V_{ohmic} - V_{act} - V_{con}$$
$$V_{open} = N_O\left[V_O + \frac{RT}{2F} ln\left(\frac{PH_2\sqrt{PO_2}}{PH_2O\sqrt{PO}}\right)\right] \quad (11)$$
$$V_{ohmic} = I_{dc}R_{FC}$$
$$V_{act} = N_O\frac{RT}{2\alpha F} ln\left(\frac{I_{dc}}{I_O}\right)$$

Where the variables are presented in the following table:

Table II. Parameter significance

		Variable	Description
R_v	Vapor gas constant	R_{H_2}	Hydrogen gas constant
R_{O_2}	Oxygen gas constant	C_{d_an}	Hydrogen purge nozzle discharge coefficient
M_v	Molar mass of vapor	$W_{sm,out}$	Mass flow exiting the supply manifold[kg/s]
k_{term}	Constants representing the linearization coefficient describing a valve[kg/(s*Pa)]	$W_{ca,out}$	Mass flow exiting the cathode[kg/s]
$W_{rm,out}$	Mass flow exiting the return manifold[kg/s]	$W_{O_2,ca,in}$	Mass flow of oxygen entering the cathode[kg/s]
$W_{H_2,reacted}$	Mass flow of oxygen reacted inside the anode[kg/s]	$\bar{R}$	Universal gas constant
$W_{O_2,reacted}$	Mass flow of oxygen in the cathode that reacts with the electrons and ions to form vapor	$W_{v,ca,gen}$	Mass flow of generated water inside the cathode

6. Control Algorithm

The MPPT can be achieved in the presence of climate variations and/or variable loads if proper control algorithms are used. Two popular algorithms are the "Perturb and Observe" (P&O) algorithm and the "Incremental Conductance" (IC) algorithm.

The P&O algorithm described in [5] has the advantage of simplicity with satisfying results in tracking. The IC algorithm computes the control law with respect to (6). If $\frac{dP}{dV} > 0$, the duty ratio increases, else if $\frac{dP}{dV} < 0$, the duty ratio decreases, otherwise the duty maintains its previous value.

However, in order to increase the performances, an IC algorithm with a variable step time is proposed. The constant step size is multiplied by $\frac{dP}{dV}$, within certain desired boundaries.

In the following scenario a PV array of 1500 watts is connected to a variable load, via a buck converter. The irradiation value changes at the half time of the simulation, from 1000 W/m^2 to 700 W/m^2, at the same time as the consumer. The performances of a P&O algorithm are compared to those of an IC with variable step size. It can be noticed that the latter converges faster towards the maximum power point and, unlike the P&O algorithm, rejects the disturbances generated by the dynamics of the load.

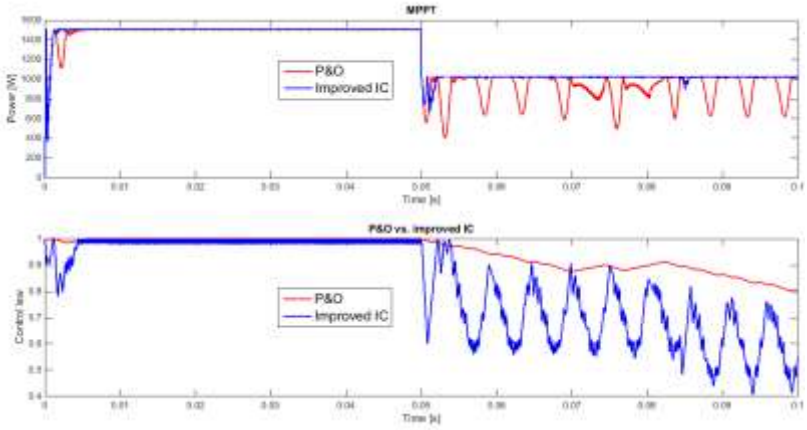

Fig. 6. Comparison between P&O and IC with variable step size.

7. Supervisory System

In this section, the supervisory system is developed and a certain test scenario is proposed. Let us presume a system composed of a PV array, a buck converter, two banks of batteries, an electrolyser, a fuel cell, and a set of variable loads. The

professional simulation software used are AMESim and Matlab. It has been shown [1]-[5] that under certain meteorological conditions, such as low irradiation or high temperature values, the PV array may not produce enough energy with respect to the consumers. The solution proposed in this article is a supervisory system that manages how the system should respond to external disturbances like variable meteorological conditions and variable loads.

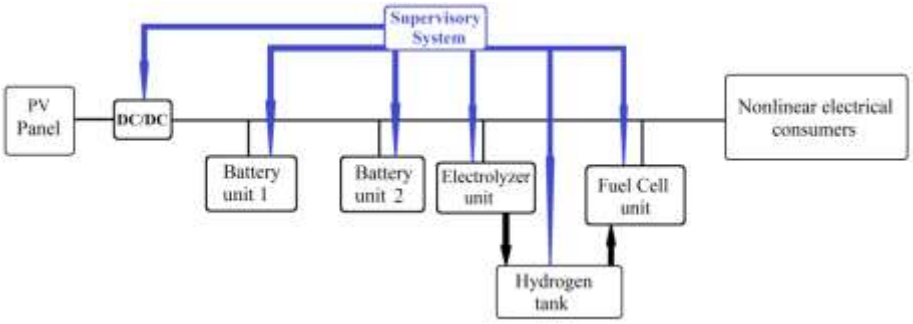

Fig. 7. System configuration.

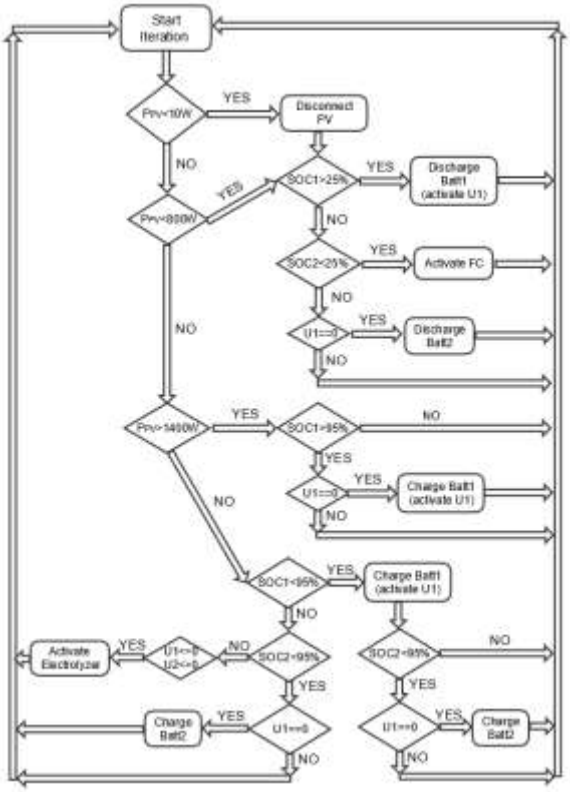

Fig. 8. System configuration.

The PV array provides energy to the consumers via the buck converter. The surplus of energy is stored first in the banks of batteries and, if the batteries are full or other conditions arise (conditions that increase the overall system performance), then through the electrolyser, the hydrogen tank is filled.

When the PV array's power becomes insufficient, the battery banks are added to the system to sustain the difference of demanded energy. In order to increase the lifespan of the batteries and to facilitate their replacement in case of failure, two sets of battery banks will be used alternatively. The first one is used, until it is fully charged or until it reaches 25% of its state of charge. Its place is taken by the second set of battery banks, which is used under similar conditions. Furthermore, a third source of energy is used whenever the state of charge of the battery banks becomes lower than 25%. The fuel cell will use the hydrogen tank to produce energy and supply it to the system. The simulations done tested the propose scenarios on a period of 10s.

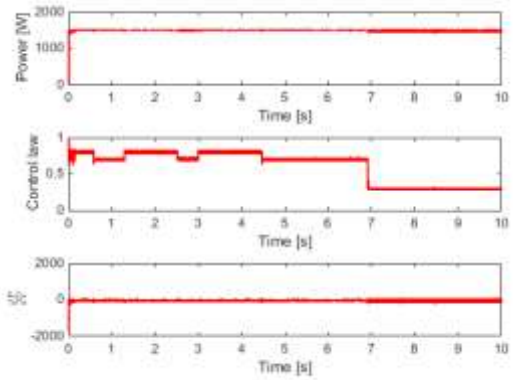

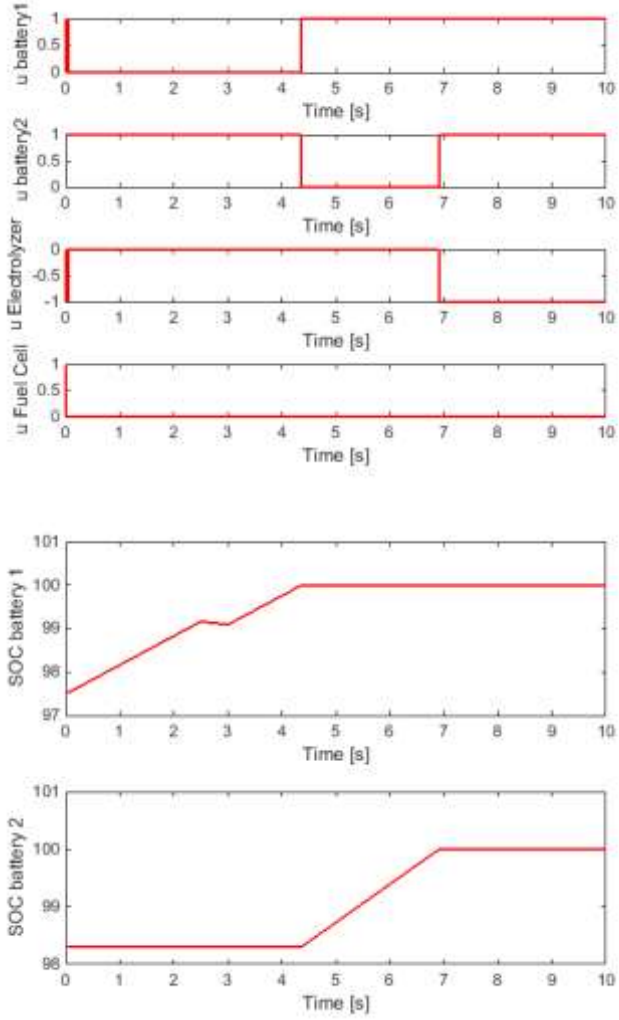

Fig. 9. Scenario 1: Different state parameter evolutions.

In the 3 figures in Fig. 9, a first scenario is shown, where a constant maximum power is maintained by means of the DC-DC converter control law described. In the battery evolution figure, one can notice the alternating functioning of the two batteries, this increasing their life-span.

At second 7, when the two batteries are fully charged, the electrolyser starts to generate hydrogen. Another important case is visible between seconds 2.5 s and 3s, when an over-demand of the consumer loads discharges the active battery 1. These consumers are nonlinear in behaviour.

In the following three figures, a scenario where there is no photovoltaic power (under 10 W).

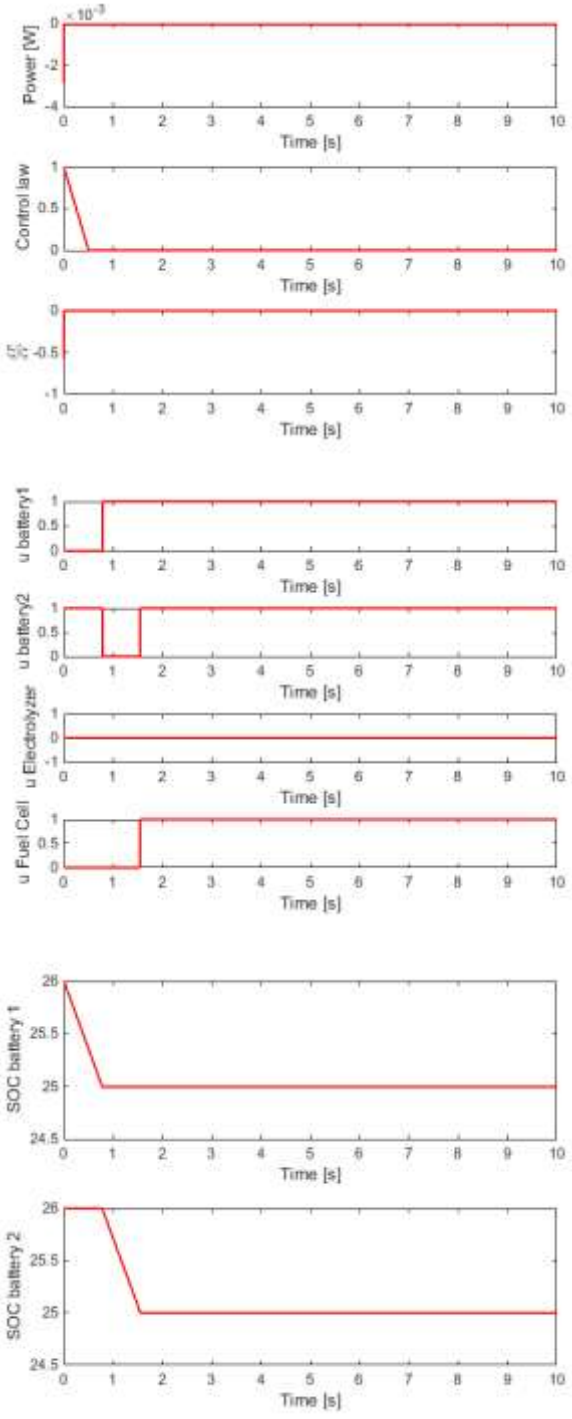

Fig. 10. Second Scenario-System parameters evolutions.

Fig.10. emphasize the tendency of the supervisor to prioritize the use of only one battery, unless it is absolutely necessary; as such, battery one starts to discharge, and battery 2 activates only when battery 1 reaches 25% state of charge at instant 0.8 s. Also, at 1.5 s, as the two batteries become depleted, the Fuel Cell is activated to compensate for the power shortage. Although not visible in the present simulations, if the hydrogen tank is filled after a certain value, the batteries will start to charge as well.

Conclusions

This article dealt with the development of an energy management system for photovoltaic sources using the concept of smart storage. The system works in an off-grid configuration, following a case scenario where storage is done at two levels: battery storage for short term and hydrogen storage for long term storage. The control system consists of a dc/dc controller and a supervisory system. The simulation platform built using the AMESim software presents itself as a good template for testing other configurations and algorithms. The topic of the paper is one of interest in this period, as a strategy for the future of the photovoltaic energy market from small and medium sources is evaluated in the research community. This paper aims to further develop the simulated models and to propose better and more complex control algorithms.

R E F E R E N C E S

[1] C. Miron, D. Popescu,A. Aitouche and N. Christov, “Observer based control for a PV system modeled by a Fuzzy Takagi Sugeno model”, in 2015 System Theory, Control and Computing, **2015** 19th International Conference, pp. 652-657.

[2] K. Ishaqu, Z. Salam, H. Taheri, “An improved two-diode photovoltaic (PV) model for PV system,” Power Electronics, Drives and Energy Systems & 2010 Power India, 2010 Joint International Conference, **2010**.

[3] N. Shannana, N.Yahayab and B. Singhc, “Single-Diode Model and Two-Diode Model of PV Modules: A Comparison,” in 2013 IEEE International Conference on Control System, Computing and Engineering, **2013**.

[4] G. Kish, J. Lee, P. Lehn, “Modelling and control of photovoltaic panels utilizing the incremental conductance method for maximum power point tracking”, IET Renewable Power Generation, **2011**.

[5] M. Villalva, J. Gazoli, and E. Filho, “Comprehensive Approach to Modeling and Simulation of Photovoltaic Arrays”, in Power Electronics, IEEE Transactions on **2009**, pp. 1198 – 1208.

[6] G. Hsief, C. Tsai and H. Hsief, "Photovoltaic Power-Increment-Aided Incremental-Conductance Maximum Power Point Tracking using Variable Frequency and Duty Controls" IEEE on Power Electronics for Distributed Generation Systems, **2012**.

[7] S. O. Amrouche, D. Rekioua and T. Rekioua, "Overview of energy storage in renewable energy systems," 2015 3rd International Renewable and Sustainable Energy Conference, Marrakech, **2015**, pp. 1-6.

[8] N. Garimella and N. K. C. Nair, "Assessment of battery energy storage systems for small-scale renewable energy integration," TENCON 2009 - 2009 IEEE Region 10 Conference, Singapore, **2009**, pp. 1-6.

[9] K. Agbossou, M. Kolhe, J. Hamelin and T. K. Bose, "Performance of a stand-alone renewable energy system based on energy storage as hydrogen," in IEEE Transactions on Energy Conversion, vol. 19, no. 3, pp. 633-640, Sept. **2004**.

[10] D. M. Ali and S. K. Salman, "A Comprehensive Review of the Fuel Cells Technology and Hydrogen Economy," *Proceedings of the 41st International Universities Power Engineering Conference*, Newcastle-upon-Tyne, **2006**, pp. 98-102.

[11] Øystein Ulleberg, "Modeling of advanced alkaline electrolyzers: a system simulation approach", International Journal of Hydrogen Energy, Volume 28, Issue 1, January **2003**, pp 21-33.

[12] Y. Wang, K. S. Chen, J. Mishler, S. C. Cho and X. C. Adroher, "A review of polymer electrolyte membrane fuel cells: Technology, applications, and needs on fundamental research", Applied Energy, Volume 88, Issue 4, April **2011**, pp. 981-1007, ISSN 0306-2619.

[13] R. Atia and N. Yamada, "Sizing and Analysis of Renewable Energy and Battery Systems in Residential Microgrids," IEEE Transactions on Smart Grid, vol. 7, no. 3, pp. 1204-1213, May **2016**.

[14] S. C. Olteanu, A. Aitouche, L. Belkoura and A. Jouni, "Embedded P.E.M. Fuel Cell Stack Nonlinear Observer by means of a Takagi-Sugeno Approach", Studies in Informatics and Control, ISSN 1220-1766, vol. 24 (1), pp. 61-70, **2015**.